

Predicting Hydraulic Conductivity of Geosynthetic Clay Liners Using a Neural Network Algorithm

Yu Tan¹; Jiannan Chen, A.M.ASCE²; and Craig H. Benson, NAE, F.ASCE³

¹Visiting Scholar, School of Engineering, Univ. of Virginia, Charlottesville, VA.

Email: yt6kd@virginia.edu

²Assistant Professor, Dept. of Civil, Environmental, and Construction Engineering, Univ. of Central Florida, Orlando, FL. Email: jiannan.chen@ucf.edu

³Dean and Hamilton Chair in Engineering, School of Engineering, Univ. of Virginia, Charlottesville, VA. Email: chbenson@virginia.edu

ABSTRACT

Hydraulic conductivity tests on geosynthetic clay liners (GCLs) to evaluate chemical compatibility can require months to years to reach equilibrium. There is a need for alternative methods to screen GCLs for chemical compatibility that are more expedient. In this study, a neural network machine learning (ML) algorithm was used to predict the hydraulic conductivity of Na-Bentonite (NaB) GCLs to leachate chemistry. Development of the ML predictive model (MLPM) included five steps: data collection, data cleaning and normalization, algorithm selection, parameters optimization, and model validation and evaluation. The MLPM is based on data collected from two decades of tests conducted on NaB GCLs with a broad range of leachates. Bentonite characteristics, permeant chemistry, and stress conditions are incorporated into the MLPM. Validation showed that the MLPM predicts hydraulic conductivity within one order of magnitude of the measured hydraulic conductivity in 85% of the cases.

INTRODUCTION

Geosynthetic clay liners (GCLs) containing sodium bentonite (NaB) are widely used as hydraulic barriers in waste containment facilities owing to their low hydraulic conductivity to water ($<10^{-10}$ m/s) (Shackelford et al. 2000, Benson et al. 2004, Salihoglu et al. 2016, Zhang et al. 2019, Rowe 2020, Tan et al. 2020). The low hydraulic conductivity (K) of NaB GCLs is achieved by the osmotic swelling of montmorillonite in NaB. Swelling of the montmorillonite fills voids within the bentonite, resulting in tortuous flow paths that lead to low hydraulic conductivity (Chen et al. 2018). Aggressive leachates (ionic strength > 300 mM) can suppress osmotic swelling, resulting in much higher hydraulic conductivity (Jo et al. 2001, Bradshaw and Benson 2014, Chen et al. 2018).

The hydraulic conductivity of GCLs is commonly measured in flexible-wall permeameters following procedures in ASTM D5084 and D6766 (ASTM 2016, 2020). These tests are often conducted on NaB GCLs with site-specific leachates to determine if low hydraulic conductivity can be achieved for the application under consideration. Testing times on the order of months to years can be required to reach the termination criteria in these tests, especially the geochemical termination criteria in D6766. Consequently, there is a need for alternative methods to assess the chemical compatibility of GCLs that are low-cost and more expedient. For example, swell index (SI) tests conducted following the ASTM D5890 (ASTM 2019) are used to evaluate how osmotic swelling of bentonite is affected by the chemistry of leachates. However, inferences

from swell index measurements require a bentonite-specific relationship between hydraulic conductivity and swell index (Kolstad et al. 2004, Chen et al. 2018). Factors such as effective stress, granule size, and mass per unit area cannot be evaluated with swell index tests. Therefore, for a given swell index, the hydraulic conductivity of GCLs can vary several orders of magnitude (Fig. 1). For example, at $SI = 10 \text{ mL/2g}$, K of NaB GCLs varies from 10^{-11} to 10^{-6} m/s under the effective stress of 20-50 kPa. The trend line in Fig. 1 corresponds to

$$K = 0.00097SI^{-5.3} \quad (1)$$

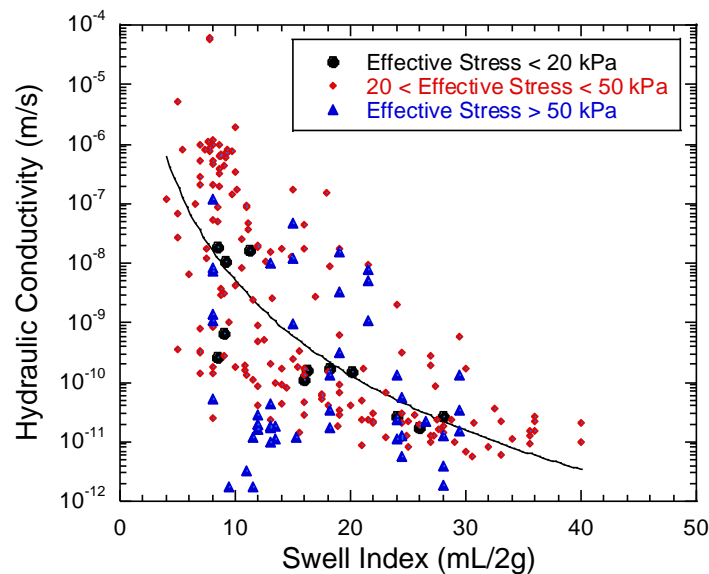


Fig. 1. Relationship between the hydraulic conductivity and swell index of NaB GCLs based on the collected dataset. Note: In the dataset, 54 points from Jo et al. (2001), 3 points from Jo et al. (2004), 2 points from Benson et al. (2004, 2007), 31 points from Kolstad et al. (2004), 9 points from Jo et al. (2005), 20 points from Lee and Shackelford (2005), 7 points from Lee et al. (2005), 26 points Katsumi et al. (2007), 2 points from Benson and Meer (2009), 4 points from Bradshaw et al. (2013), 6 points from Bradshaw and Benson (2014), 8 points from Scalia et al. (2014), 12 points from Bradshaw et al. (2016), 6 points from Tian et al. (2016), 7 points from Setz et al. (2017), and 42 points from Chen et al. (2018).

Machine learning (ML) is an alternative method to estimate the hydraulic conductivity of NaB GCLs for site-specific leachates while accounting for multi factors that influence hydraulic conductivity. ML algorithms use a map of correlations between an independent variable (e.g., hydraulic conductivity) and dependent variables (e.g., leachate chemical variables, effective stress, granule size, etc.) to make a prediction, which allows the consideration of comprehensive effects on the hydraulic conductivity of NaB GCLs. This relatively new technique has been applied successfully to geotechnical engineering (Phoon 2020) for predicting soil permeability (Araya and Ghezzehei, 2019, Koltar et al. 2019), saturated water content (Szabó et al. 2019), and tunnel behavior (Kovačević et al. 2020).

In this study, an ML predictive model (MLPM) was developed to predict the hydraulic conductivity of NaB GCLs using fourteen impact factors (independent parameters) that are commonly measured for GCLs. The impact factors were partitioned into three groups: bentonite

characteristics, permeant chemistry, and stress conditions. A database comprised of hydraulic conductivity and ancillary measurements (describing impact factors) was compiled from the literature to support MLPM development. The database was used to train a neural network algorithm to predict the hydraulic conductivity of NaB GCLs.

METHODS

Database with the Hydraulic Conductivity of NaB GCLs and Its Impact Factors. Data describing the hydraulic conductivity of NaB GCLs and 14 impact factors were collected from seventeen different sources published within the last two decades, all of which are listed in the citation for Fig. 1. All of the hydraulic conductivity tests were conducted in flexible-wall permeameters following the falling-head methods in ASTM D5084 and D6766 (ASTM 2016, 2020). The impact factors on hydraulic conductivity include bentonite characteristics [montmorillonite content, cation exchange capacity (CEC), bound cation fractions, mass per unit area, and D_{50} granule size], permeant chemistry (ionic strength and concentrations of major monovalent and polyvalent cations and anions), and effective stress. Data from more than twenty different commercially available NaB GCLs were included in the database, with CEC of the bentonite ranging from 63 to 93 cmol^+/kg and montmorillonite content ranging from 51% to 88%. GCLs with granular and powdered bentonite were included in the database. The permeant solutions consisted of deionized water, municipal solid waste leachates, coal combustion product leachates, radioactive waste leachates, and salt solutions with a broad range of ionic strength (0 to 3000 mM). Data were collected from tests conducted at average effective stresses ranging from 10 to 520 kPa.

ML algorithm. The neural network algorithm was used in this study to construct the MLPM. The neural network mimics the way that the human brain operates to create interconnected neurons (Dongare et al. 2012), as presented in Fig. 2. The impact factors were used as input neurons (a set of neurons $\{x_i|x_1, x_2, \dots, x_m\}$), and the hydraulic conductivity of NaB GCLs ($f(x)$) was set as output. Between the input and output neurons, one or more layers of neurons, i.e., the hidden layers, were inset to transfer information. Different weights were applied to the connection between each neuron to represent the importance of the neurons in the previous layer to the receiving neuron. For example, neuron a_1 summed the values from the input layer with the weights (w) of each neuron (i.e., $w_1x_1 + w_2x_2 + \dots + w_mx_m$). The hyperbolic tan function was applied to the sum values in order to include a non-linear relationship between each layer. The values of the neurons in the last hidden layers were received by the output layer and transformed into output values. The square error (i.e., the loss) of the whole network was calculated by comparing the output values and the corresponding measured hydraulic conductivities. To optimize the output, Limited-memory Broyden–Fletcher–Goldfarb–Shanno algorithm (L-BFGS) was used to minimize the loss by repeatedly updating the weight matrices. The iterations stop when the decrease in loss below a specific number or the preset maximum number of iterations is reached.

Machine learning predictive model. The following procedure was used to create MLPM:

- 1) **Data cleaning:** Data of different magnitude affect the model learning process differently. Non-negative and non-zero data were normalized to 0~1 by a $L2$ norm:

$$L2 \text{ norm} = \sqrt{m_1^2 + m_2^2 + \dots + m_n^2} \quad (2)$$

where m_1 , m_2 , and m_n are the original values of one impact factor. The normalized values were obtained by the ratio between the original value and the L_2 norm (i.e., m_n/L_2 norm). Then, the

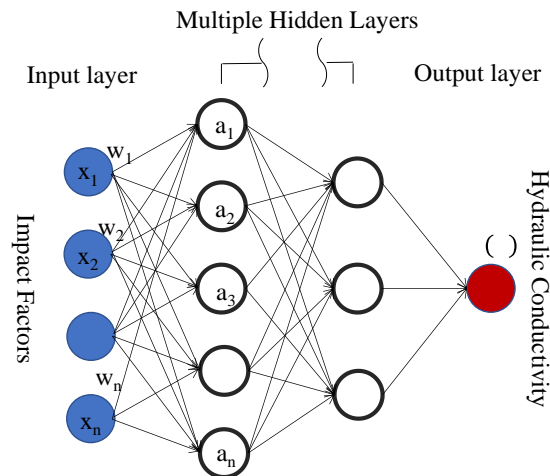


Fig. 2. Illustration of multiple hidden layers neural network model.

- 2) **Algorithm selection:** Agyare et al. (2007) developed a neural network model for predicting the hydraulic conductivity of natural soil tested on two pilot sites. Soil properties such as sand, silt, and clay content, bulk density, and organic carbon, were used as the model inputs. The model presented reliable estimations when the input data were normalized to 0-1. The neural network algorithm used in this study followed a similar approach developed by Agyare et al. (2007). The code and model parameters are introduced elaborately in the Sklearn website (https://scikit-learn.org/stable/modules/generated/sklearn.neural_network.MLPRegressor.html#).
- 3) **Parameter optimization:** The model parameters, such as the number of hidden layers, the used loss functions, and the maximum number of iterations, were optimized by cross-validation. The ranges of each model parameter were predefined based on experiences. Then, the model tested all candidate parameters in the ranges to calculate the mean squared error (MSE) of the regression. The parameters that achieved the minimum MSE of the model were selected as the optimum parameters. The log-transformed mean squared error (LMSE) was used instead of typical MSE to determine the optimization for hydraulic conductivity. The LMSE was calculated based on the predicted and measured hydraulic conductivity of NaB GCLs log-transformed forms. Additionally, the training data were randomly split into five consecutive folds (subsets) during the optimization instead of using the whole training dataset. Each of the five folds could be held for validation while the other folds were used for model training for iterations. This approach enhanced the reuse of data and avoided over-fitting.
- 4) **Model validation and evaluation:** The model was validated by predicting hydraulic conductivities for each of the cases in the validation data set using the corresponding impact parameters, and then comparing the predicted hydraulic conductivities to the measured hydraulic conductivities in the validation data set. The performance of the

model was evaluated by the ratio between the predicted and measured hydraulic conductivity of GCLs in the validation data set. The ratio is higher than one when the predicted hydraulic conductivity exceeds the measured hydraulic conductivity (conservative prediction) and lower than one when the predicted hydraulic conductivity is less than the measured hydraulic conductivity (unconservative prediction). The range of unconservative prediction was pointed, which range should be cautious for the application under consideration.

RESULTS

The comparison between the predicted (by the MLPM, K_p) and measured (K_m) hydraulic conductivities in the validation data set is shown in Fig. 3. The red dashed lines correspond to a 10-fold difference between the predicted and measured hydraulic conductivities, whereas the blue dashed lines correspond to a 100-fold difference. In the validation dataset (total 60 measurements), 87% of the predicted hydraulic conductivities fall within the 10-fold range and 97% within the 100-fold range. Only two predictions fall outside the 100-fold (114 times higher and 103 time lower) range. The data also exhibit no apparent bias, with the predicted hydraulic conductivities are on average within a 3-fold (i.e., $10^{0.48}$) difference from the measured hydraulic conductivities.

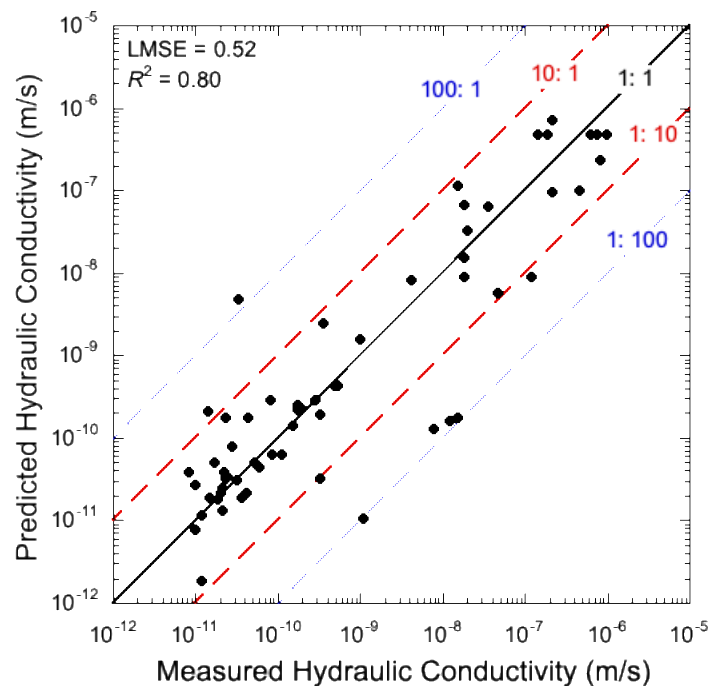


Fig. 3. Comparison of MLPM predicted and measured hydraulic conductivities based on the testing dataset for model validation.

The ratio of predicted and measured hydraulic conductivities in the validation data set is shown in Fig. 4 as a function of the measured hydraulic conductivity. Hydraulic conductivities were also predicted based on the swell index using Equation 1 and are shown in Fig. 4. In general, the ratio is smaller for the predictions made with the MLPM compared to that of the

swell index. Only 46% of the swell index predicted hydraulic conductivities fall within the 10-fold range comparing to the measured hydraulic conductivity, which is lower than the 87% achieved by the MLPM prediction. In addition, the LMSE of the swell index prediction (LMSE = 1.39) is 2.7-times higher than that of the MLPM prediction (LMSE = 0.52).

The trained and validated MLPM above was issued as a tool to predict the hydraulic conductivity of NaB GCLs. This model can be run in a Python environment and predict the hydraulic conductivity based on bentonite characteristics, permeant chemistry, and effective stress (i.e., the impact factors as model inputs). The prediction presented high reliability to screen out the NaB GCLs with high hydraulic conductivity ($K > 10^{-8}$ m/s) since the predicted K is all higher than 10^{-10} m/s in the validation data set. When the GCL with a hydraulic conductivity around 10^{-10} m/s, the ratio of predicted and measured hydraulic conductivities varied from 0.1 to 100 (Fig. 4). The ratio indicates that the measured hydraulic conductivity of the GCL could vary from 10^{-8} to 10^{-11} m/s. Thus, a hydraulic conductivity test is still suggested for the GCL.

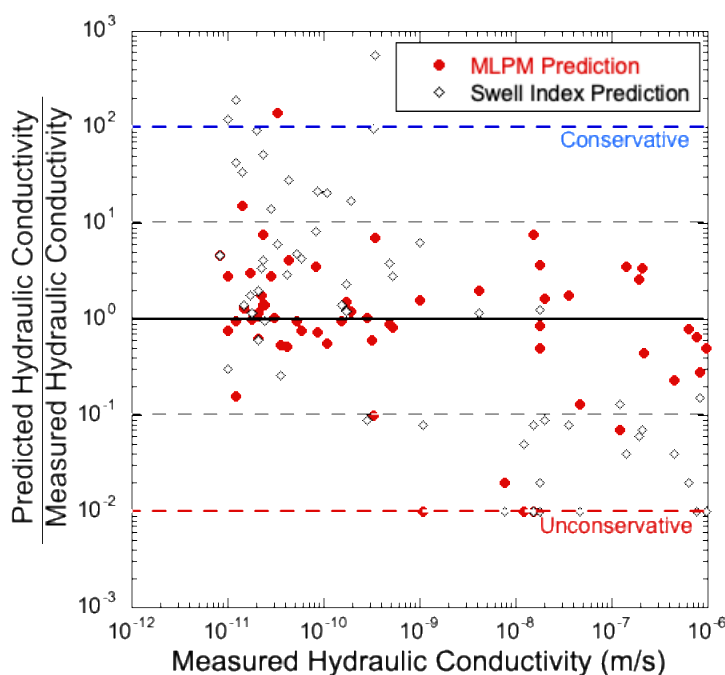


Fig. 4. The ratio of predicted and measured hydraulic conductivities using MLPM and swell index.

SUMMARY AND CONCLUSIONS

A predictive model was developed using machine learning to predict the hydraulic conductivity of NaB GCLs using 14 commonly measured and controlled parameters. A database containing 239 hydraulic conductivity measurements of various types of NaB GCLs to a wide range of permeant solutions and effective stress was used for calibration and validation of the model. Validation of the model indicated that 87% of the predicted hydraulic conductivities were within 10-fold of the measured hydraulic conductivities, and 97% within a 100-fold difference. Predictions made with ML method are more precise than predictions made based on the swell index.

REFERENCES

- Araya, S. N., and Ghezzehei, T. A. (2019). "Using Machine Learning for Prediction of Saturated Hydraulic Conductivity and Its Sensitivity to Soil Structural Perturbations." *Water Resources Research*, 55(7), 5715-5737.
- Agyare, W. A., Park, S. J., and Vlek, P. L. G. (2007). "Artificial Neural Network Estimation of Saturated Hydraulic Conductivity." *Vadose Zone J.*, 6(2), 423-431.
- ASTM. (2016). *Standard Test Methods for Measurement of Hydraulic Conductivity of Saturated Porous Materials Using a Flexible Wall Permeameter*. ASTM D5084, West Conshohocken, PA.
- ASTM. (2020). *Standard Test Method for Evaluation of Hydraulic Properties of Geosynthetic Clay Liners Permeated with Potentially Incompatible Aqueous Solutions*. ASTM D6766, West Conshohocken, PA.
- ASTM. (2019). *Standard Test Method for Swell Index of Clay Mineral Component of Geosynthetic Clay Liners*. ASTM D5890, West Conshohocken, PA.
- Benson, C. H., Jo, H. Y., and Abichou, T. (2004). "Forensic analysis of excessive leakage from lagoons lined with a composite GCL." *Geosynthetics International*, 11(3), 242-252.
- Benson, C. H., Thorstad, P. A., Jo, H. Y., and Rock, S. A. (2007). "Hydraulic Performance of Geosynthetic Clay Liners in a Landfill Final Cover." *Journal of Geotechnical and Geoenvironmental Engineering*, 133(7), 814-827.
- Benson, C. H., and Meer, S. R. (2009). "Relative Abundance of Monovalent and Divalent Cations and the Impact of Desiccation on Geosynthetic Clay Liners." *Journal of Geotechnical and Geoenvironmental Engineering*, 135(3), 349-358.
- Bradshaw, S. L., and Benson, C. H. (2014). "Effect of Municipal Solid Waste Leachate on Hydraulic Conductivity and Exchange Complex of Geosynthetic Clay Liners." *Journal of Geotechnical and Geoenvironmental Engineering*, 140(4), 04013038.
- Bradshaw, S. L., Benson, C. H., and Scalia, J. (2013). "Hydration and Cation Exchange during Subgrade Hydration and Effect on Hydraulic Conductivity of Geosynthetic Clay Liners." *Journal of Geotechnical and Geoenvironmental Engineering*, 139(4), 526-538.
- Bradshaw, S. L., Benson, C. H., and Rauen, T. L. (2016). "Hydraulic Conductivity of Geosynthetic Clay Liners to Recirculated Municipal Solid Waste Leachates." *Journal of Geotechnical and Geoenvironmental Engineering*, 142(2), 04015074.
- Chen, J., Benson, C. H., and Edil, T. B. (2018). "Hydraulic Conductivity of Geosynthetic Clay Liners with Sodium Bentonite to Coal Combustion Product Leachates." *Journal of Geotechnical and Geoenvironmental Engineering*, 144(3), 04018008.
- Dongare, A. D., Kharde, R. R., and Kachare, A. D. (2012). "Introduction to artificial neural network." *International Journal of Engineering and Innovative Technology (IJEIT)*, 2(1), 189-194.
- Jo, H. Y., Benson, C. H., and Edil, T. B. (2004). "Hydraulic Conductivity and Cation Exchange in Non-prehydrated And Prehydrated Bentonite Permeated with Weak Inorganic Salt Solutions." *Clays and Clay Minerals*, 52(6), 661-679.
- Jo, H. Y., Benson, C. H., Shackelford, C. D., Lee, J.-M., and Edil, T. B. (2005). "Long-Term Hydraulic Conductivity of a Geosynthetic Clay Liner Permeated with Inorganic Salt Solutions." *Journal of Geotechnical and Geoenvironmental Engineering*, 131(4), 405-417.
- Jo, H. Y., Katsumi, T., Benson, C. H., and Edil, T. B. (2001). "Hydraulic Conductivity and Swelling of Nonprehydrated GCLs Permeated with Single-Species Salt Solutions." *Journal of Geotechnical and Geoenvironmental Engineering*, 127(7), 557-567.

- Katsumi, T., Ishimori, H., Ogawa, A., Yoshikawa, K., Hanamoto, K., and Fukagawa, R. (2007). "Hydraulic conductivity of nonprehydrated geosynthetic clay liners permeated with inorganic solutions and waste leachates." *Soils and Foundations*, 47(1), 79-96.
- Kolstad, D. C., Benson, C. H., and Edil, T. B. (2004). "Hydraulic Conductivity and Swell of Nonprehydrated Geosynthetic Clay Liners Permeated with Multispecies Inorganic Solutions." *Journal of Geotechnical and Geoenvironmental Engineering*, 130(12), 1236-1249.
- Kotlar, A. M., Iversen, B. V., and de Jong van Lier, Q. (2019). "Evaluation of Parametric and Nonparametric Machine-Learning Techniques for Prediction of Saturated and Near-Saturated Hydraulic Conductivity." *Vadose Zone J.*, 18(1), 180141.
- Kovačević, M. S., Bačić, M., and Gavin, K. (2020). "Application of neural networks for the reliability design of a tunnel in karst rock mass." *Canadian Geotechnical Journal*, 58(4), 455-467.
- Lee, J. M., and Shackelford, C. D. (2005). "Impact of Bentonite Quality on Hydraulic Conductivity of Geosynthetic Clay Liners." *Journal of Geotechnical and Geoenvironmental Engineering*, 131(1), 64-77.
- Lee, J. M., Shackelford, C. D., Benson, C. H., Jo, H. Y., and Edil, T. B. (2005). "Correlating Index Properties and Hydraulic Conductivity of Geosynthetic Clay Liners." *Journal of Geotechnical and Geoenvironmental Engineering*, 131(11), 1319-1329.
- Phoon, K.-K. (2020). "The story of statistics in geotechnical engineering." *Georisk: Assessment and Management of Risk for Engineered Systems and Geohazards*, 14(1), 3-25.
- Rowe, R. K. (2020). "Geosynthetic clay liners: Perceptions and misconceptions." *Geotextiles and Geomembranes*, 48(2), 137-156.
- Salihoglu, H., Chen Jiannan, N., Likos William, J., and Benson Craig, H. "Hydraulic Conductivity of Bentonite-Polymer Geosynthetic Clay Liners in Coal Combustion Product Leachates." *Geo-Chicago 2016*, 438-447.
- Scalia, J., Benson, C. H., Bohnhoff, G. L., Edil, T. B., and Shackelford, C. D. (2014). "Long-Term Hydraulic Conductivity of a Bentonite-Polymer Composite Permeated with Aggressive Inorganic Solutions." *Journal of Geotechnical and Geoenvironmental Engineering*, 140(3), 04013025.
- Setz, M. C., Tian, K., Benson, C. H., and Bradshaw, S. L. (2017). "Effect of ammonium on the hydraulic conductivity of geosynthetic clay liners." *Geotextiles and Geomembranes*, 45(6), 665-673.
- Shackelford, C. D., Sevick, G. W., and Eykholt, G. R. (2010). "Hydraulic conductivity of geosynthetic clay liners to tailings impoundment solutions." *Geotextiles and Geomembranes*, 28(2), 149-162.
- Szabó, B., Szatmári, G., Takács, K., Laborczi, A., Makó, A., Rajkai, K., and Pásztor, L. (2019). "Mapping soil hydraulic properties using random-forest-based pedotransfer functions and geostatistics." *Hydrol. Earth Syst. Sci.*, 23(6), 2615-2635.
- Tan, Y., Zhang, H. Y., and Wang, Y. (2020). "Evaporation and shrinkage processes of compacted bentonite-sand mixtures." *Soils and Foundations*, 60(2), 505-519.
- Tian, K., Benson, C. H., and Likos, W. J. (2016). "Hydraulic conductivity of geosynthetic clay liners to low-level radioactive waste leachate." *Journal of Geotechnical and Geoenvironmental Engineering*, 142(8), 04016037.
- Zhang, H., Tan, Y., Zhu, F., He, D., and Zhu, J. (2019). "Shrinkage property of bentonite-sand mixtures as influenced by sand content and water salinity." *Construction and Building Materials*, 224, 78-88.